

# Pre-clinical characterization of the novel Fibroblast Activation Protein (FAP) targeting ligand PNT6555 for the imaging and therapy of cancer

Robin M. Hallett<sup>1</sup>, Sarah E. Poplawski<sup>2</sup>, Kyle E. Novakowski<sup>1</sup>, Mark H. Dornan<sup>1</sup>, Shin Hye Ahn<sup>3</sup>, Shuang Pan<sup>2</sup>, Wu Wengen<sup>2</sup>, Liu Yuxin<sup>2</sup>, David G. Sanford<sup>2</sup>, Valerie S. Hergott<sup>1</sup>, Quang-De Nguyen<sup>3</sup>, Anthony P. Belanger<sup>3</sup>, Jack H. Lai<sup>2</sup>, William W. Bachovchin<sup>2</sup>, Joe A. B. McCann<sup>1</sup>

<sup>1</sup>Point Biopharma Inc, Indianapolis, IN, <sup>2</sup>Tufts University, Boston, MA, <sup>3</sup>Dana-Farber Cancer Institute, Boston, MA

AACR AGM 2022  
Abstract ID: 3554

## Introduction

### Fibroblast Activation Protein (FAP- $\alpha$ )

- Fibroblast Activation Protein- $\alpha$  (FAP- $\alpha$ ) is a compelling pan cancer target for imaging and therapy as it is overexpressed in >90% of epithelial tumors<sup>1</sup>.
- In cancer, FAP is highly expressed on cancer associated fibroblasts (CAFs)<sup>2</sup>, which drive tumor progression and resistance to chemo and immunotherapy<sup>3,4,5</sup>.
- FAP shows limited expression in adult normal tissues<sup>6</sup>.
- FAP positivity based on FAP targeted PET imaging has been demonstrated in all major tumor types<sup>7</sup>.
- POINT Biopharma has developed PNT6555, a FAP-targeting small molecule with high selectivity for FAP, for the diagnosis and treatment of FAP-avid solid tumors.

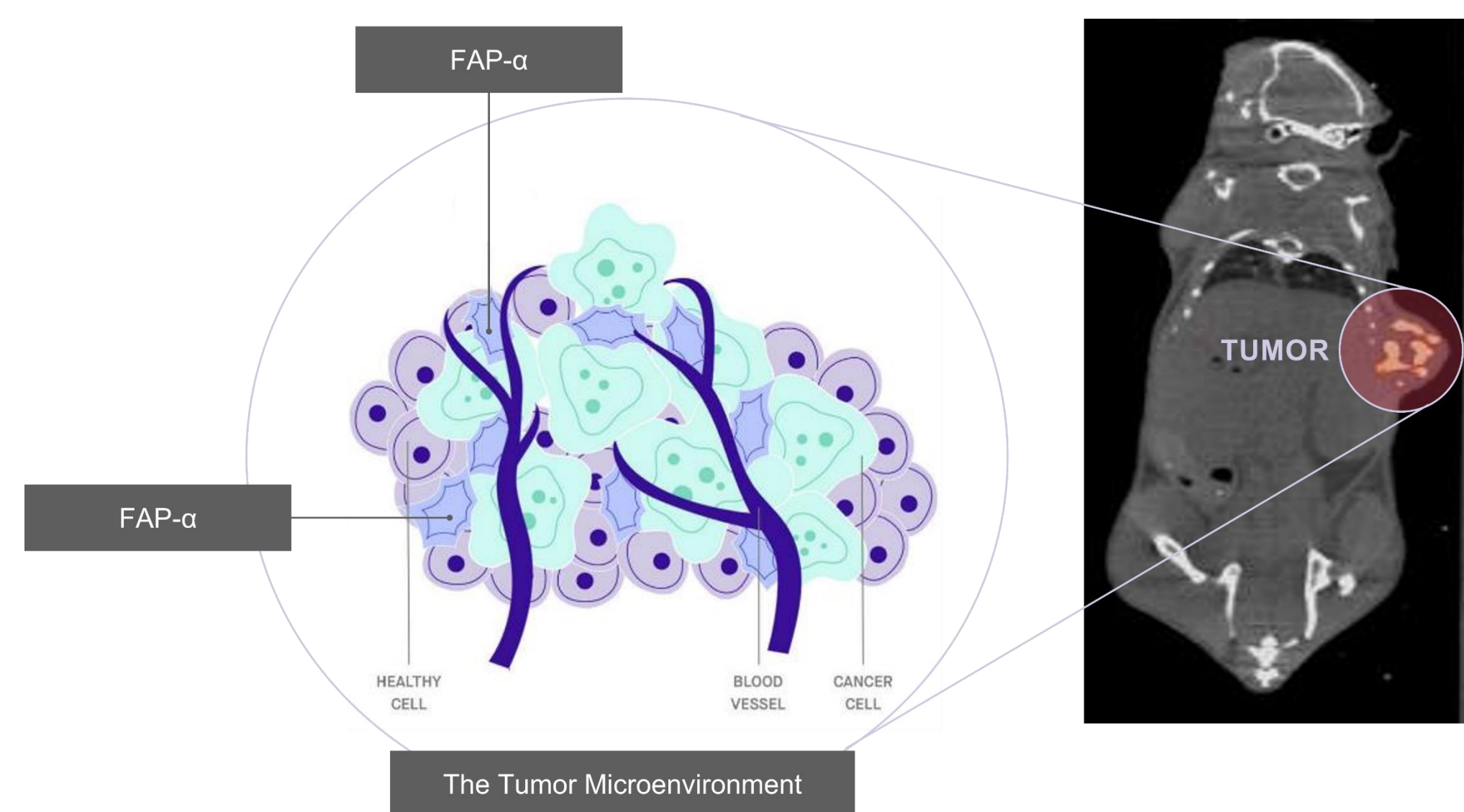


Figure 1: Schematic representation of the FAP-expressing CAFs in the tumor microenvironment.

### PNT6555

- PNT6555 comprises a DOTA chelator (1,4,7,10-tetraazacyclododecane-1,4,7,10-tetraacetic acid) and a FAP-targeting moiety (Bz-D-Ala-boroPro) connected via an aminomethyl linker.
- Gallium-68 is chelated to PNT6555 for diagnostic purposes and lutetium-177 or actinium-225 is chelated to PNT6555 for therapeutic purposes.

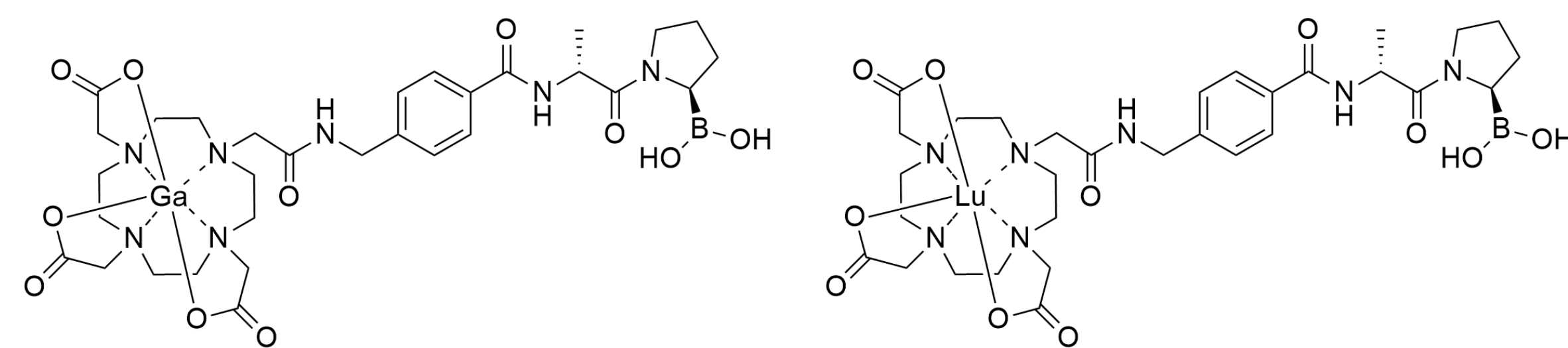


Figure 2: The corresponding (Ga/Lu)-DOTA-AmBz-D-Ala-boroPro chelates represent the imaging and therapeutic theranostic pair of PNT6555.

## Materials & Methods

- Biochemistry:** Potency ( $IC_{50}$ ) and enzyme specificity studies were performed using soluble FAP/DPP4/PREP derived from either recombinant protein or human serum. Murine FAP was expressed on HEK 293 cells (HEK-mFAP). FAP/DPP4/PREP inhibition was measured using fluorogenic FAP/DPP4/PREP substrates and measuring the release of the fluorescent cleavage product. Non-radioactive (natural) gallium and lutetium isotopes were used for all *in vitro* studies.
- Animal experiments:** All animal experiments were approved by the Dana-Farber Cancer Institute Animal Care and Use Committee. For HEK-mFAP tumor xenograft studies, Male Fox Chase SCID mice were purchased from Charles River Laboratories at 6-8 weeks old and allowed to acclimate for 1 week. All mice were housed under standard care conditions and monitored weekly. Tumors were established by subcutaneous injection of  $5 \times 10^6$  cells into the right flank in 100  $\mu$ L PBS.
- Tumor growth:** Tumor growth was monitored weekly with caliper measurements (tumor volume = length  $\times$  width<sup>2</sup>  $\times$  0.5). Study endpoints include tumor size > 2 cm in any dimension, tumor ulceration, mouse is moribund, and > 15% body weight lost from the last measurement.
- PET/SPECT studies:** PET and SPECT imaging studies were performed using a dedicated small animal PET/CT / SPECT/CT scanner with animals under gaseous anesthesia. Following a 7.4 MBq bolus injection (IV) of <sup>68</sup>Ga-PNT6555, Dynamic PET scans were performed in list mode format over 60 min, followed by image reconstruction in FORE/3D-OSEM-MAP. Low dose CT scans were performed for anatomical reference and to segment and extract volume of interest-derived standardized uptake values (SUVs).
- Biodistribution studies:** Biodistribution studies were performed at defined time points following a 7.5 MBq bolus injection (IV) of <sup>177</sup>Lu-PNT6555. Tissue samples were counted for radioactivity on a Cobra-II Auto-Gamma counter and data was expressed as injected dose per gram (%ID/g).
- Efficacy:** Efficacy studies were performed using HEK-mFAP tumor bearing male Fox Chase SCID mice. Mice were treated with a single bolus (IV) injection of either <sup>177</sup>Lu-PNT6555 or <sup>225</sup>Ac-PNT6555 and monitored for tumor volume and survival.

## Results

### PNT6555 potently and specifically inhibits FAP

- PNT6555, cold Ga-labelled PNT6555 and cold Lu-labelled PNT6555 potently inhibited FAP (Figure 3, Table 1).
- A high degree of specificity for FAP was also demonstrated for PNT6555 as compared to the related enzymes PREP and DPPIV (Figure 4, Table 2).

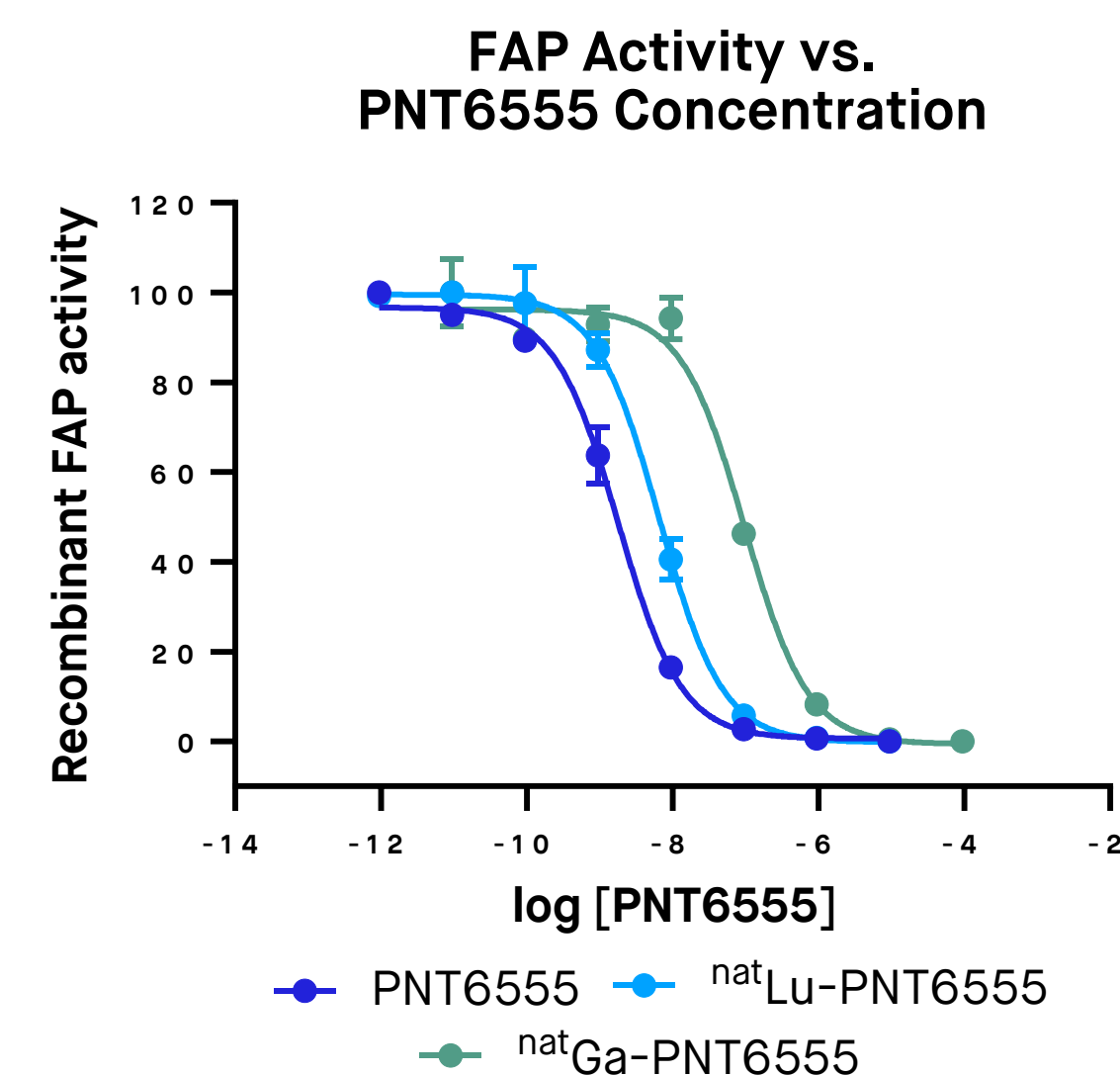


Figure 3:  $IC_{50}$  dose inhibition curves for FAP protease activity with PNT6555.

Table 1: Potency of PNT6555 and <sup>nat</sup>Lu/<sup>nat</sup>Ga-PNT6555 on inhibition of human FAP.

Inhibitor	Recombinant Human FAP	Human Serum FAP	HEK-mFAP
	$IC_{50}$ (nM)	$IC_{50}$ (nM)	$IC_{50}$ (nM)
PNT6555	$1.8 \pm 0.4$	$2.5 \pm 0.4$	$0.8 \pm 0.03$
<sup>nat</sup> Lu-PNT6555	$6.6 \pm 0.5$	$10 \pm 1.7$	$1.2 \pm 0.1$
<sup>nat</sup> Ga-PNT6555	$98 \pm 5.4$	$100 \pm 9.3$	$47 \pm 5.9$

### Enzyme Activity vs. PNT6555 Concentration

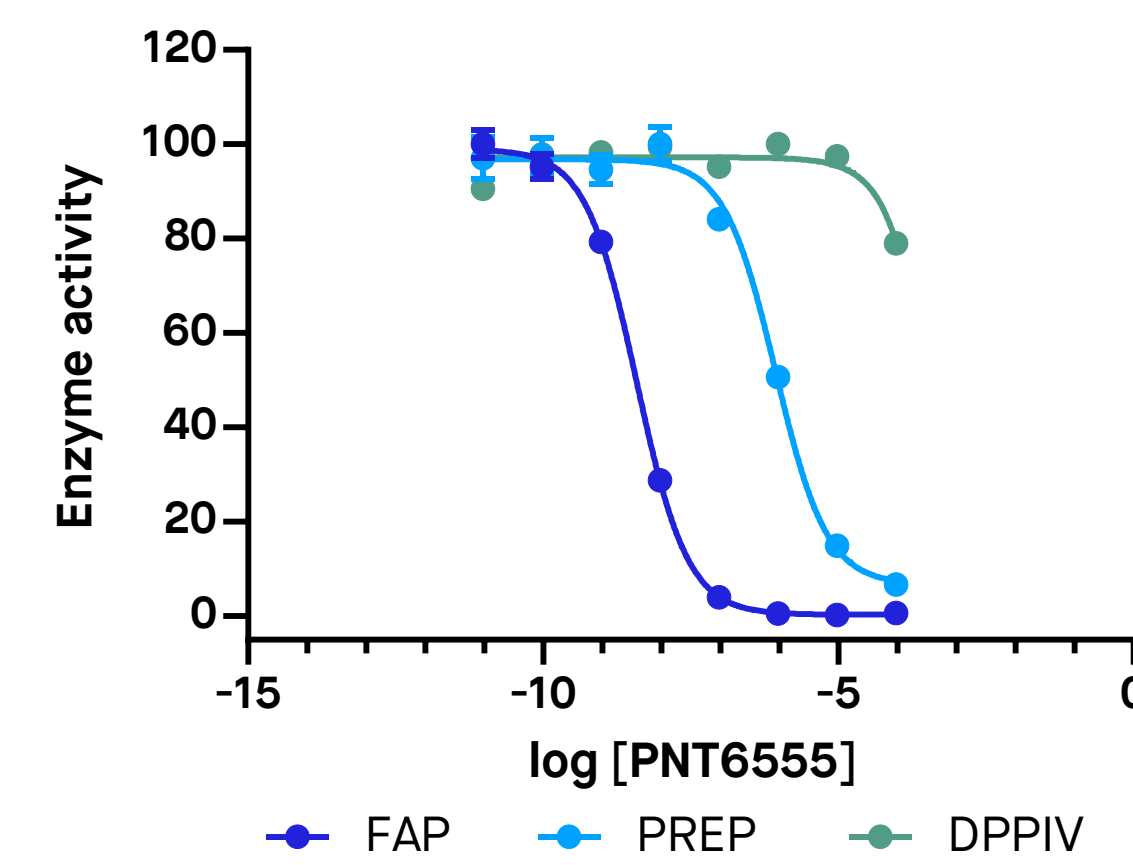


Figure 4:  $IC_{50}$  dose inhibition curves for FAP, PREP and DPPIV with PNT6555.

Table 2: Selectivity indices of PNT6555 and <sup>nat</sup>Lu/<sup>nat</sup>Ga-PNT6555 on inhibition of PREP and DPPIV.

Inhibitor	PREP Selectivity Index	DPPIV Selectivity Index
PNT6555	500	>55000
<sup>nat</sup> Lu-PNT6555	621	>15000
<sup>nat</sup> Ga-PNT6555	37	>10000

### In vivo biodistribution of <sup>68</sup>Ga-PNT6555

- Based on SUVmean, <sup>68</sup>Ga-PNT6555 uptake in the blood peaked at 4.3 (SEM: 0.26) at 0.375 min post-injection and subsequently showed a continuous decrease throughout the imaging interval to 0.3 (SEM 0.03) at 57.5 min.
- Kidney uptake peaked at 3.84 (SEM 1.02) at 2.5 min post-injection and decreased to 0.76 (SEM 0.01) at 57.5 min.
- The tumor was the only tissue of increasing uptake throughout the imaging interval, with very limited uptake into normal tissues and rapid clearance through the kidneys and into the bladder.

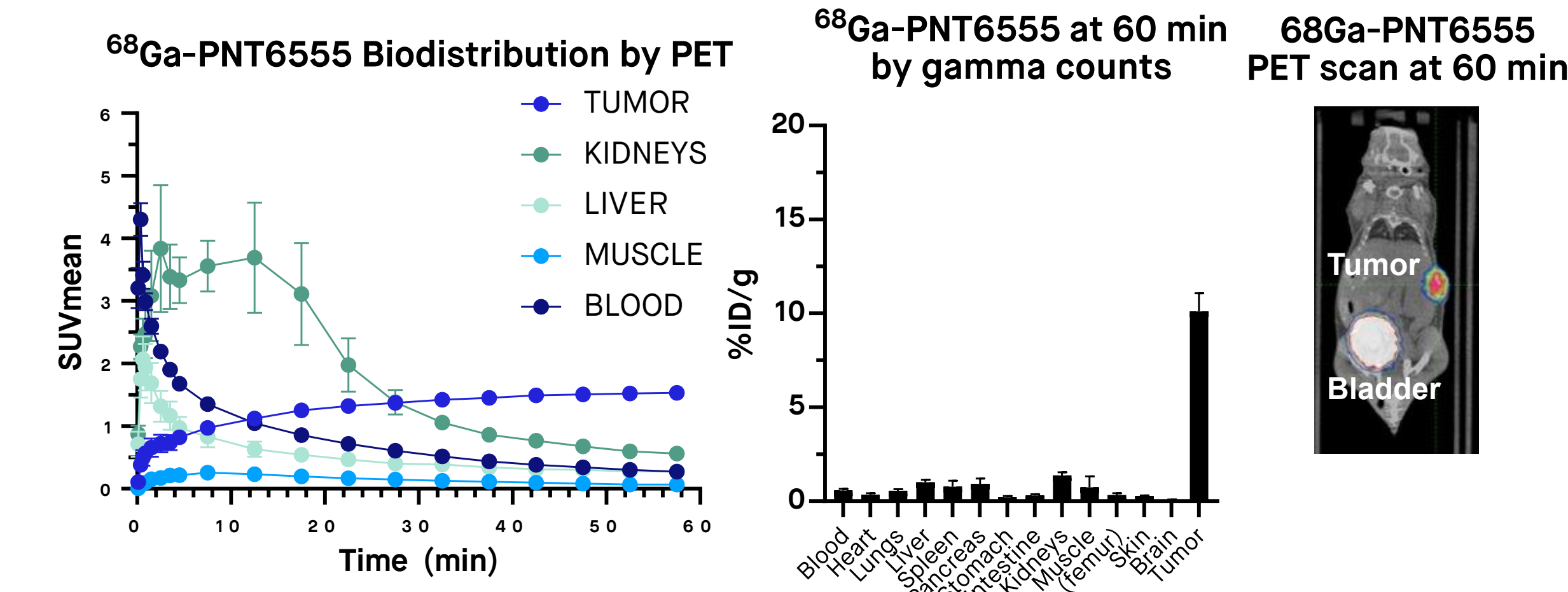


Figure 5: (Left) Biodistribution of <sup>68</sup>Ga-PNT6555 in HEK-mFAP tumor-bearing mice was assessed by dynamic PET imaging. (Middle) Direct organ assay by gamma-counting in tissues collected at 60 min necropsy. (Right) PET image taken at 60 min.

## Results (Ctd.)

### In vivo biodistribution of <sup>177</sup>Lu-PNT6555

- SPECT:** <sup>177</sup>Lu-PNT6555 was cleared rapidly through the kidneys into the bladder, with significant activity observed in the bladder at 3h (35.76 %ID/mL, SEM: 9.45) and 24h (3.4 %ID/mL, SEM: 1.84).
- Biodistribution:** Very limited retention was observed in normal tissues. Tumor showed prolonged retention out to 168h (11.41 %ID/g, SEM: 1.71).

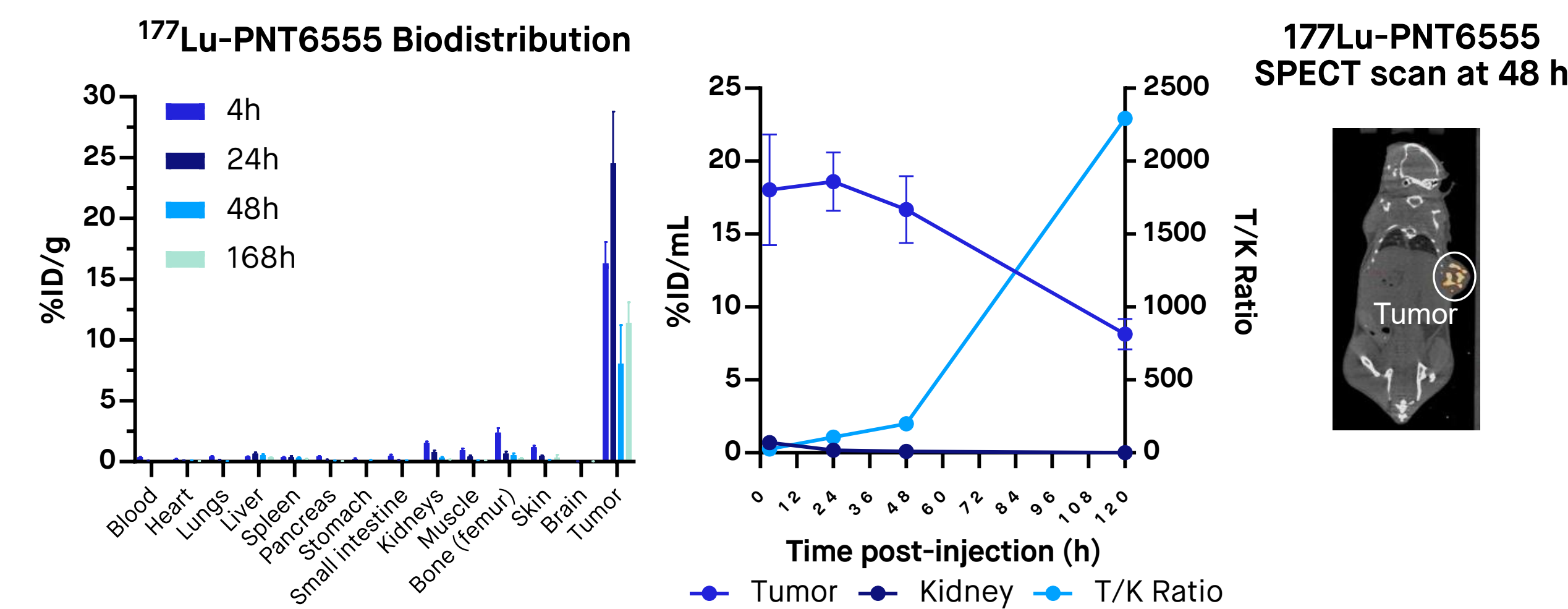


Figure 6: (Left) Biodistribution of <sup>177</sup>Lu-PNT6555 by direct organ assay in HEK-mFAP tumor-bearing mice in tissues collected at indicated timepoints. (Middle) Tissue distribution assessed by SPECT imaging in tumor and kidney tissues and the tumor:kidney ratio of %ID/mL across the experimental time course. (Right) SPECT image taken at t=48h.

### In vivo efficacy of <sup>177</sup>Lu-PNT6555

- Dose-dependent tumor regression was observed, with significant benefits to survival.
- 6/6 mice treated at 60 MBq and 3/6 mice treated at 30 MBq showed complete and durable tumor regression.
- There was no evidence of declines in body weight in any treatment group.

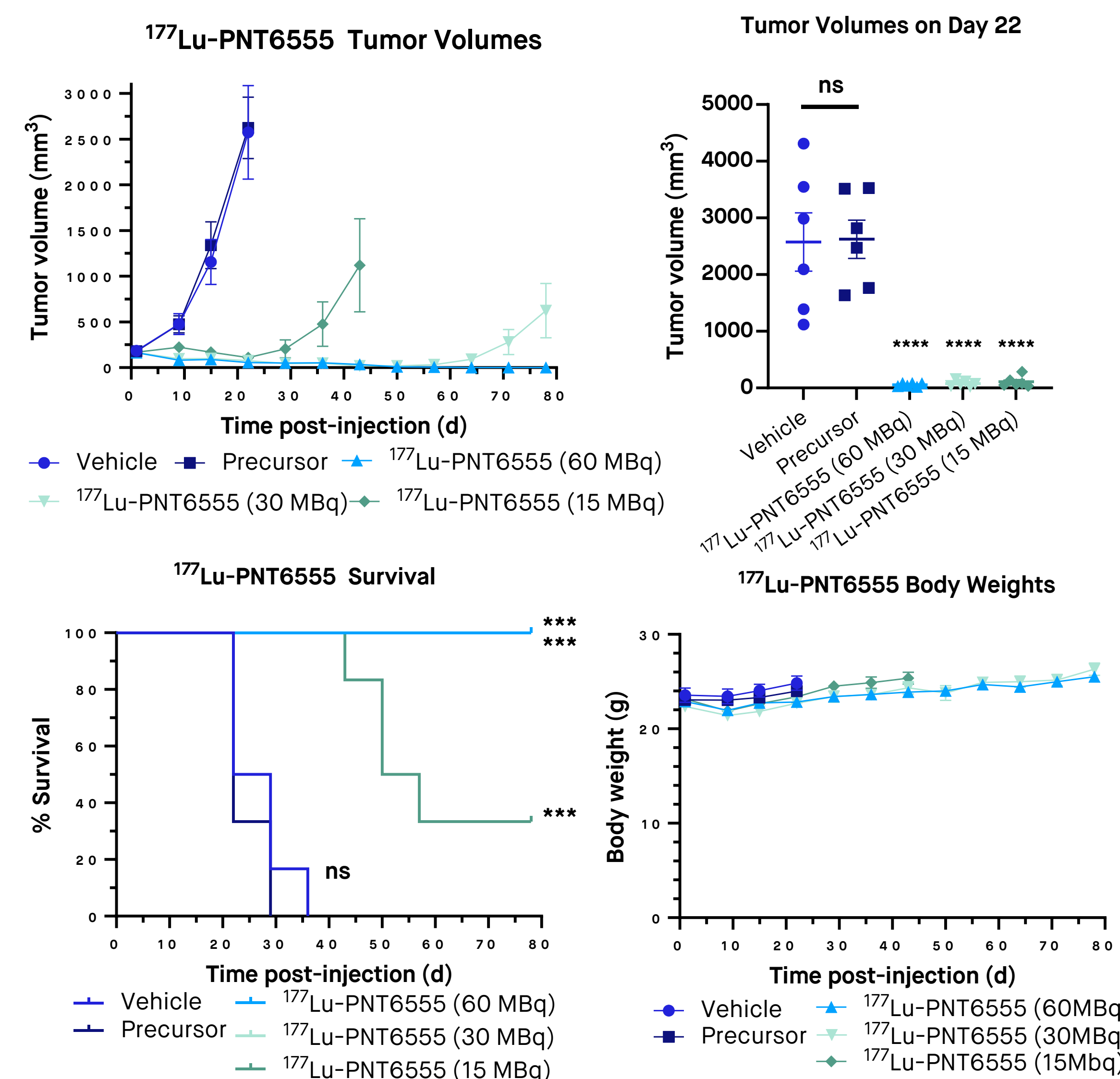


Figure 7: The capacity of <sup>177</sup>Lu-PNT6555 to inhibit the growth of HEK-mFAP tumor-bearing mice. (Top Left) Tumor volume was determined until day 78 by weekly caliper measurements. Tumor volumes are shown until the first mouse reached endpoint. (Top Right) Tumor volumes at the date of the first mouse reaching endpoint \*\*\*  $p < 0.0001$ , one way ANOVA. (Bottom Left) Survival curves are shown until day 78 post-injection. \*\*\*  $p < 0.001$ , Log-rank test. (Bottom Right) Body weights shown until day 78 post-injection.

## Results (Ctd.)

### In vivo efficacy of <sup>225</sup>Ac-PNT6555

- Dose-dependent tumor regression was observed, with significant increases in survival.
- 4/6 mice treated at 50 kBq showed complete and durable tumor regression.
- There was no evidence of declines in body weight associated with treatment.

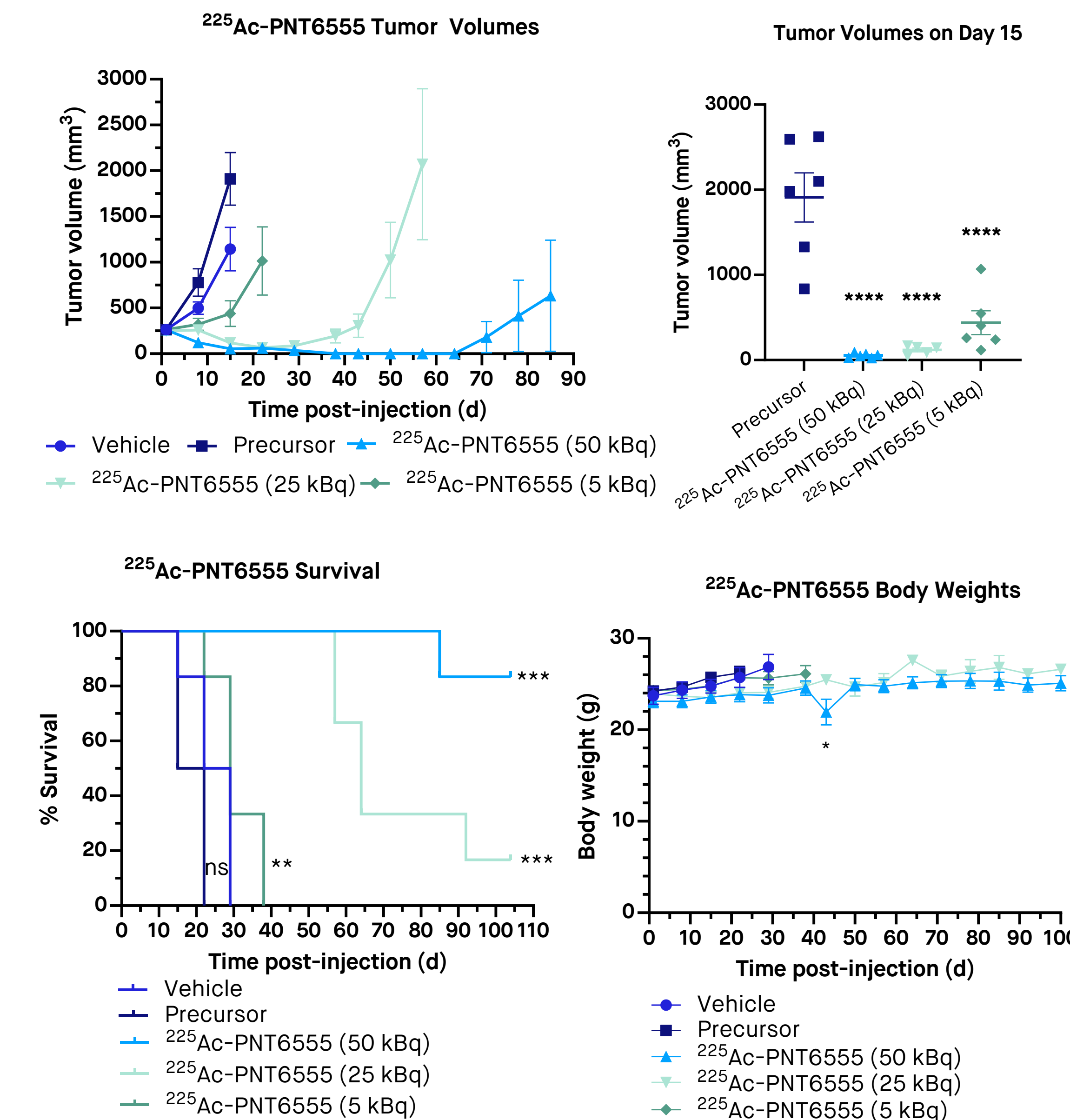


Figure 8: The capacity of <sup>225</sup>Ac-PNT6555 to inhibit the growth of HEK-mFAP tumor-bearing mice. (Top Left) Tumor volume was determined until day 85 by weekly caliper measurements. Tumor volumes are shown until the first mouse reached endpoint. (Top Right) Tumor volumes at the date of the first mouse reaching endpoint \*\*\*\*  $p < 0.0001$ , one way ANOVA. (Bottom Left) Survival curves are shown until day 104 post-injection. \*\*  $p < 0.01$ , \*\*\*  $p < 0.001$ , Log-rank test. (Bottom Right) Body weights shown until day 100 post-injection. Star indicates water bottle leak in a single cage of 3 mice in the 50 kBq group.

## Conclusions

- PNT6555 shows nanomolar potency against human and murine FAP and high selectivity over closely-related targets.
- <sup>68</sup>Ga-PNT6555 is an effective imaging agent, with strong tumor targeting, low background in normal tissues and rapid clearance via urinary excretion.
- <sup>177</sup>Lu-PNT6555 shows prolonged tumor retention out to 168 h post-injection.
- Efficacy studies of <sup>177</sup>Lu-PNT6555 and <sup>225</sup>Ac-PNT6555 demonstrate compelling, dose-responsive inhibition of HEK-mFAP tumor growth.
- Clinical studies are planned using <sup>68</sup>Ga-PNT6555 for imaging and <sup>177</sup>Lu-PNT6555 for therapy.

## References

- Mhawech-Fauceglia P. *et al.* 2015. Cancer Microenviron.
- Jacob M. *et al.* 2012. Curr. Mol. Med.
- Mariathasan S. *et al.* 2018. Nature
- Domen A. *et al.* 2021. Cancers
- Joshi RS. *et al.* 2021. Cancers
- Niedermeyer J. *et al.* 2001. Int J. Dev.
- Kratovich C. *et al.* 2019. J. Nucl. Med.

## Disclosures

R.M. Hallett: Point Biopharma. S.E. Poplawski: Bach Biosciences. K.E. Novakowski: Point Biopharma. M.H. Dornan: Point Biopharma. S. Ahn: None. S. Pan: Bach Biosciences. W. Wengen: Bach Biosciences. L. Yuxin: Bach Biosciences. D.G. Sanford: Bach Biosciences. V.S. Hergott: Point Biopharma. Q. Nguyen: None. A.P. Belanger: None. J.H. Lai: Bach Biosciences. W. Bachovchin: Bach Biosciences; Avacta; Point Biopharma. J.A.B. McCann: Point Biopharma.

